iScience

CellPress
OPEN ACCESS

Article

Third-generation taxanes SB-T-121605 and SB-T-121606 are effective in pancreatic ductal adenocarcinoma

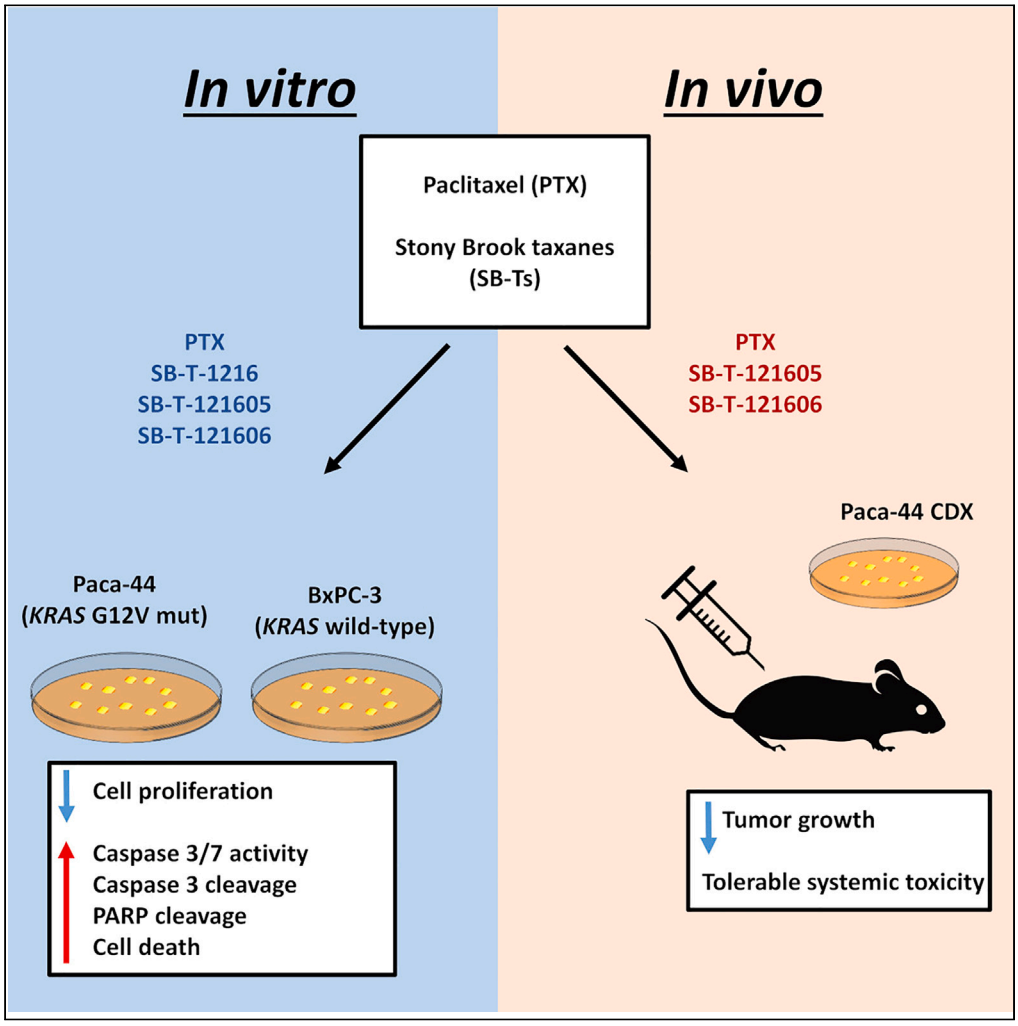

Tomas Sychra, Alzbeta Spalenkova, Stepan Balatka, ..., Iwao Ojima, Martin Oliverius, Pavel Soucek

pavel.soucek@szu.cz

Highlights

Study explored effects of experimental taxanes in pancreatic cancer models

Stony Brook taxanes SB-T-1216, 121605, and 121606 were cytostatic *in vitro*

Mechanism was comparable in Paca-44 *KRAS* G12V mutated and BxPC-3 wild type *in vitro*

The combination of SB-T-121606 with paclitaxel had the best antitumor effect *in vivo*

Sychra et al., iScience 27, 109044
February 16, 2024
https://doi.org/10.1016/j.isci.2024.109044

iScience

CellPress
OPEN ACCESS

Article

Third-generation taxanes SB-T-121605 and SB-T-121606 are effective in pancreatic ductal adenocarcinoma

Tomas Sychra,[1,2] Alzbeta Spalenkova,[3,4] Stepan Balatka,[3,4] Radka Vaclavikova,[3,4] Karolina Seborova,[3,4] Marie Ehrlichova,[3,4] Jaroslav Truksa,[5] Cristian Sandoval-Acuña,[5] Vlasta Nemcova,[6] Arpad Szabo,[2,7] Kamila Koci,[2] Tereza Tesarova,[3,4] Lei Chen,[8] Iwao Ojima,[8] Martin Oliverius,[1,2] and Pavel Soucek[3,4,9,*]

SUMMARY

Pancreatic cancer is a severe malignancy with increasing incidence and high mortality due to late diagnosis and low sensitivity to treatments. Search for the most appropriate drugs and therapeutic regimens is the most promising way to improve the treatment outcomes of the patients. This study aimed to compare (1) *in vitro* efficacy and (2) *in vivo* antitumor effects of conventional paclitaxel and the newly synthesized second (SB-T-1216) and third (SB-T-121605 and SB-T-121606) generation taxanes in *KRAS* wild type BxPC-3 and more aggressive *KRAS* G12V mutated Paca-44 pancreatic cancer cell line models. *In vitro*, paclitaxel efficacy was 27.6 ± 1.7 nM, while SB-Ts showed 1.7–7.4 times higher efficacy. Incorporation of SB-T-121605 and SB-T-121606 into *in vivo* therapeutic regimens containing paclitaxel was effective in suppressing tumor growth in Paca-44 tumor-bearing mice at small doses (≤3 mg/kg). SB-T-121605 and SB-T-121606 in combination with paclitaxel are promising candidates for the next phase of preclinical testing.

INTRODUCTION

Pancreatic cancer is predicted to become the second most common cause of cancer-related death by 2030.[1] Its morbidity and mortality increase year by year, becoming a rising threat to the common population. Yet, it remains one of the most poorly understood malignancies.[2]

The most common form of pancreatic carcinoma (90%) is pancreatic ductal adenocarcinoma (PDAC), followed by less frequent squamous cell, acinar, mucinous, neuroendocrine carcinomas, and their combinations. The PDAC tumor microenvironment consists of both extracellular matrix components and fibroblastic, vascular, and immune cells that support tumor growth and provide a barrier against drug delivery.[3] PDAC risk factors remain not completely defined but currently known ones can be divided into modifiable and unmodifiable. Modifiable factors are health-contributing factors such as obesity, smoking, diet, and alcohol consumption while unmodifiable ones originate in those aspects of our life we cannot influence, such as ethnicity, sex, or hereditary genetic predispositions such as the *BRCA1*, *BRCA2*, or *PALB2* mutations.[4] One of the most perplexing current trends is an increase in PDAC incidence and mortality in high-income regions.[5] Furthermore, on a molecular level, *KRAS* is the predominant gene mutated in PDAC, resulting in the fact that its mutations can be found in nearly all PDACs. Therefore, this type of cancer is the most RAS–addicted.[6]

One of the only possible curative options is surgical resection followed by adjuvant chemotherapy (unless contraindicated).[7] Chemotherapy in patients is commonly prescribed according to the performance status (PS) of the patient; the higher the PS, the more aggressive chemotherapy can be applied. There are options from mFOLFIRNOX (leucovorin calcium, fluorouracil, irinotecan hydrochloride, and oxaliplatin) in patients with high PS to FOLFOX (leucovorin calcium, fluorouracil, and oxaliplatin) or gemcitabine with nab-paclitaxel or with capecitabin in worsening PS and gemcitabine alone as a last resort.[8]

As previously mentioned, taxane (nab-paclitaxel) is one of the therapies of choice in combination with gemcitabine, especially in metastatic PDAC patients.[9] Taxanes block the disassembly of cellular microtubules during cell division and restrict proliferation, migration, and metastasis.[10] A family of synthetic derivatives of conventional taxanes was created, also known as the Stony Brook Taxane derivatives (SB-Ts), by the laboratory of Prof. Iwao Ojima (Institute of Chemical Biology & Drug Discovery, New York University at Stony Brook, NY, USA).

[1]Department of Surgery, University Hospital Kralovske Vinohrady, 100 00 Prague, Czech Republic
[2]Third Faculty of Medicine, Charles University, 100 00 Prague, Czech Republic
[3]Toxicogenomics Unit, National Institute of Public Health, 100 00 Prague, Czech Republic
[4]Laboratory of Pharmacogenomics, Biomedical Center, Faculty of Medicine in Pilsen, Charles University, 323 00 Pilsen, Czech Republic
[5]Institute of Biotechnology of the Czech Academy of Sciences, BIOCEV Research Center, 252 50 Vestec, Czech Republic
[6]Department of Biochemistry, Cell and Molecular Biology, Third Faculty of Medicine, Charles University, 100 00 Prague, Czech Republic
[7]Department of Pathology University Hospital Kralovske Vinohrady, 100 00 Prague, Czech Republic
[8]Institute of Chemical Biology & Drug Discovery, State University of New York at Stony Brook, Stony Brook, NY 11794-3400, USA
[9]Lead contact
*Correspondence: pavel.soucek@szu.cz
https://doi.org/10.1016/j.isci.2024.109044

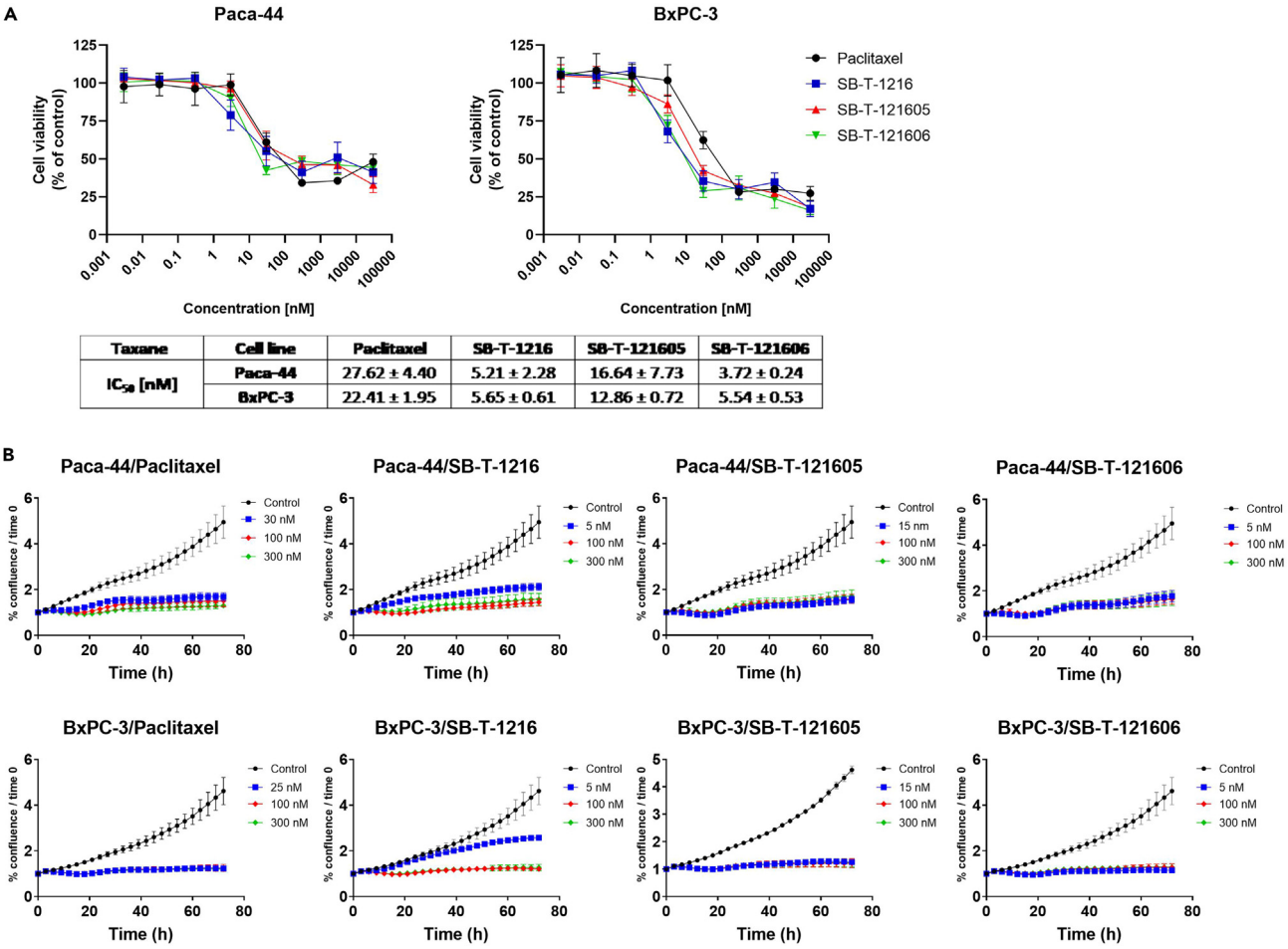

Taxane	Cell line	Paclitaxel	SB-T-1216	SB-T-121605	SB-T-121606
IC_{50} [nM]	Paca-44	27.62 ± 4.40	5.21 ± 2.28	16.64 ± 7.73	3.72 ± 0.24
	BxPC-3	22.41 ± 1.95	5.65 ± 0.61	12.86 ± 0.72	5.54 ± 0.53

Figure 1. *In vitro* efficacy of paclitaxel and SB-Ts

(A) Graph showing the cell viability (% of control cells) of Paca-44 and BxPC-3 cell line treated with paclitaxel (PTX), second- and third-generation of SB-Ts for 72 h. Table with IC_{50} values as mean ± S.D. of three independent experiments presented.

(B) Representative graphs depicting the effect of concentrations corresponding to IC_{50} (5–30 nM) 100 nM and 300 nM of PTX, SB-T-121605, and SB-T-12606 on cellular proliferation in Paca-44 and BxPC-3 cells. The data are presented as mean ± standard deviation of two independent experiments.

These are taxanes with modifications at the C-2, C-10, and C-3′ structure positions of PTX (Figure S1).[11] We have found that second-generation SB-T-1216 downregulates the Hedgehog[12] and *KRAS* signaling pathways *in vivo*.[13] The third-generation SB-T-121605 and SB-T-121606 have even better metabolic stability and membrane permeability to cancerous cells, and thus it is possible to use them in lower concentrations. Recently, they have shown exciting effectiveness in PTX-resistant ovarian carcinoma models both *in vitro* and *in vivo*.[14]

This study aimed to compare the effectiveness of second-generation SB-T (SB-T-1216) and its corresponding derivatives of the third-generation (SB-T-121605 and SB-T-121606) with parent drug PTX in *in vitro* models of PDAC - pancreatic cell lines Paca-44 and BxPC-3 differing by *KRAS* mutation status and cell line-derived mouse xenografts (CDX) based on *KRAS* G12V mutant Paca-44 *in vivo*. The *in vivo* efficacy of SB-Ts was assessed in a combination regimen with PTX, as shown by us previously in ovarian cancer models,[14] and compared to PTX alone. This report demonstrates that combined regimens of conventional PTX with third-generation SB-Ts are effective in aggressive pancreatic carcinoma *in vivo*.

RESULTS

Paclitaxel and SB-Ts decrease cell proliferation of Paca-44 and BxPC-3 cells *in vitro*

The effect of PTX and SB-Ts was analyzed via the calculation of IC_{50} values. The efficacy of all examined taxanes was very similar in both tested cell lines. The most effective taxane was SB-T-121606 with the IC_{50} value of 3.72 ± 0.24 nM in Paca-44 cells and 5.54 ± 0.53 nM in BxPC-3 cell line. The efficacy of SB-T-1216 was very similar (IC_{50} 5.21 ± 2.28 nM for Paca-44 and 5.65 ± 0.61 nM for BxPC-3 cells) and higher than another third-generation SB-T-121605 (16.64 ± 4.73 nM and 12.86 ± 0.72 nM for Paca-44 and BxPC-3, respectively). All tested SB-Ts were more effective than PTX (IC_{50} 27.62 ± 1.40 nM and 22.41 ± 1.95 nM for Paca-44 and BxPC-3 cell lines, respectively. (Figure 1A) However, unlike in our

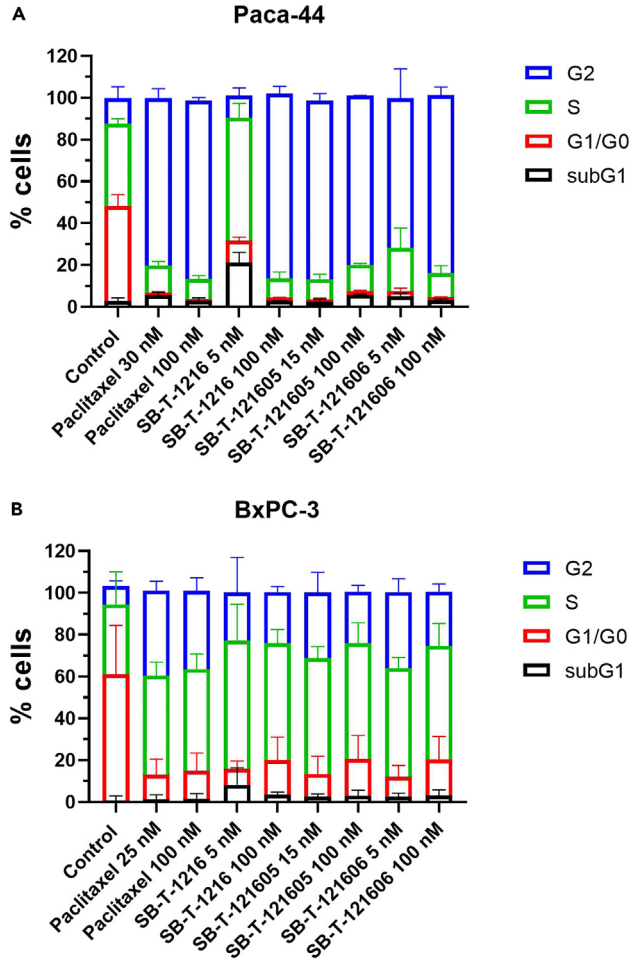

Figure 2. Cell cycle changes after 24 h of incubation of cells with paclitaxel and experimental SB-Ts *in vitro*

(A and B) Taxane concentrations corresponding to IC_{50} values (5–30 nM) and 100 nM concentration were used in (A) Paca-44, (B) BxPC-3 cell line. Histograms display three independent experiments as mean ± SD.

study analyzing PTX-resistant ovarian cancer cells NCI/ADR-RES,[14] where SB-Ts at the highest concentrations after 72 h of incubation caused a reduction in cell viability to 3.6–4.3% of the control, the same incubation time led to the reduction of the Paca-44 cell line viability to 48.1 ± 4.3%, 41.3 ± 6.2%, 33.0 ± 4.3%, and 44.4 ± 1.8% for PTX, SB-T-1216, SB-T-121605, and SB-T-121606, respectively. The viability of BxPC-3 cells was reduced to 27.3 ± 3.7%, 17.1 ± 4.2%, 18.2 ± 1%, and 16.1 ± 2.2% for PTX, SB-T-1216, SB-T-121605, and SB-T-121606, respectively.

Cellular proliferation in the presence of PTX, SB-T-1216, SB-T-121605, and SB-T-121606 was determined by real-time monitoring of cellular confluence using Incucyte SX3. All compounds showed a marked cytostatic effect (Figure 1B) even at the lowest tested concentration, corresponding to IC_{50} values (5–30 nM for Paca-44 and 5–25 nM for BxPC-3 cells), confirming previous results. Original video files allowing the real–time inspection of cell proliferation are part of the supplementary materials (Videos S1, S2, S3, S4, S5, S6, S7, S8, S9, and S10).

SB-Ts are effective in blocking the cell cycle of Paca-44 and BxPC-3 cells

Cell cycle changes were analyzed by flow cytometry at 24 h of incubation of the Paca-44 and BxPC-3 cell lines with PTX or SB-Ts. The incubation of Paca-44 cells with 100 nM of PTX or each SB-T individually caused a G2/M block of the cell cycle. Treatment with lower concentrations (corresponding to respective IC_{50} values) caused the G2/M block in case of all taxanes, except for SB-T-1216, for which a higher amount of cells in subG1 phase and S phase was detected (Figures 2A and S2). The BxPC-3 cell line was affected differently by PTX and all SB-Ts. The percentage of cells in the G2/M phase was increased when compared to control. However, a major proportion of cells - 49% when incubated with 100 nM PTX, 55% with 100 nM SB-T-1216, 55% with 100 nM SB-T-121605 and 54% with 100 nM SB-T-121605 (compared to 33% of control cells) - was found in the S phase of the cell cycle (Figures 2B and S3). However, the detection of phosphorylated Bcl-2 protein (P-Bcl-2), that is connected to mitotic arrest,[15] was more evident in the BxPC-3 cell line when compared to Paca-44, which had almost no P-Bcl-2 detected (Figures 3A and 3B).

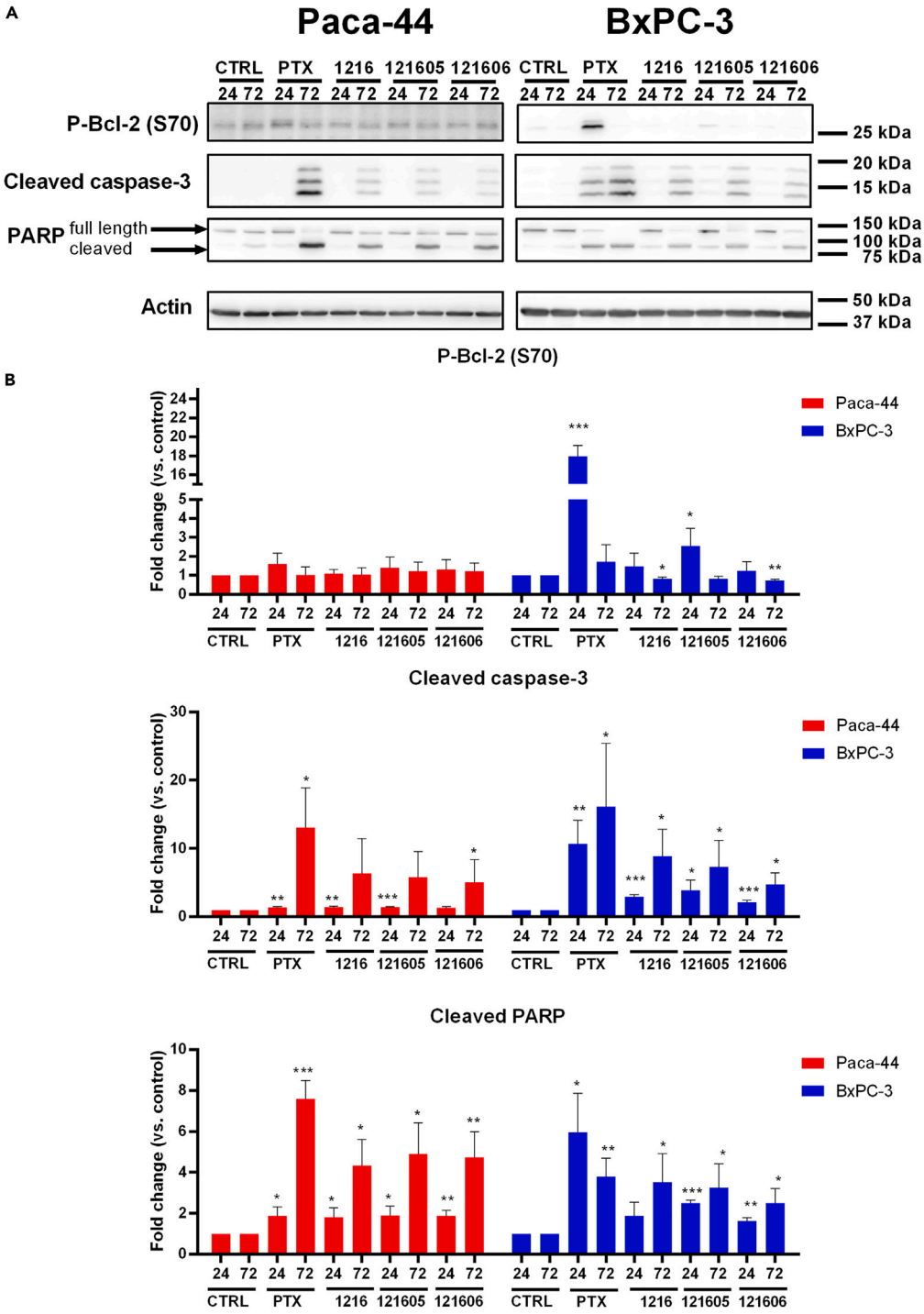

Figure 3. Western blot analysis of phospho-Bcl-2 (P-Bcl-2), PARP and cleaved caspase-3 expression in Paca-44 and BxPC-3 cells after paclitaxel and SB-Ts treatment

(A) Cells treated with 25 nM (BxPC-3) or 30 nM (Paca-44) PTX, 5 nM SB-T-1216 (1216), 15 nM SB-T-121605 (121605), 5 nM SB-T-121606 (121606) or fresh medium without taxanes (CTRL) for 24 and 72 h. Expression of P-Bcl-2 (Ser70), PARP, and cleaved caspase-3 was analyzed employing western blot and relevant antibodies. Actin was used as a loading control. Data of one representative experiment out of three independent experiments shown.

(B) Densitometric analysis of P-Bcl-2 (Ser70), cleaved form of PARP, and cleaved caspase-3. Data expressed as fold change of the respective control cells after 24 h and 72 h of treatment. The mean ± SD of three independent experiments shown. *p < 0.05, **p < 0.01, ***p < 0.001.

Temporal disparity in taxane effects observed in BxPC-3 compared to Paca-44 cells

To gain a deeper understanding of how SB-Ts affect the pancreatic cell lines, we analyzed the induction of cell death. The real-time analysis of cell death on Incucyte SX3, conducted continuously over a period of 72 h, showed a significant number of dead cells in the first 24 h of incubation of the BxPC-3 cell line with tested taxanes. All tested compounds caused cell death at 100 and 300 nM concentrations and PTX and third generation SB-Ts caused a similar effect also at concentrations corresponding to their IC_{50}. Second-generation SB-T-1216 showed a weaker effect at the 5 nM concentration. However, in Paca-44, we detected almost no dead cells during 72 h of monitoring (Figure 4A), even at high taxane concentrations (100 and 300 nM). Moreover, the analysis of cell death by Annexin V has not shown an increase in percentage of dead Paca-44 cells after 24 h, but in the BxPC-3 cell line, we observed a significantly higher increased number of dead cells for all tested taxanes and concentrations, except for 5 nM SB-T-1216. After 72 h of incubation, there was an increase in both cell lines (Figures 4B, S4, and S5). Original video files allowing the real-time inspection of cell death are part of the supplementary materials (Videos S1, S2, S3, S4, S5, S6, S7, S8, S9, and S10). Consistently, our findings demonstrated no significant changes in caspase 3/7 activity in the presence of tested taxanes in the Paca-44 cell line after 24 h, but in BxPC-3, the activity was significantly increased (up to 1150% of control cells). After 72 h, the activity was significantly increased in both cell lines (Figure 4C). Accordingly, the immunoblot detection of cleaved caspase-3 and PARP protein in cells incubated with IC_{50} concentrations of tested compounds showed the cleavage after 24 h in BxPC-3, but in Paca-44 cells, the cleavage was evident after 72 h of incubation (Figures 3A and 3B). Collectively these data suggest notably delayed cell death induction in Paca-44 compared to BxPC-3 underlying the effect of PTX or SB-Ts incubation.

Small doses of SB-Ts have a strong antitumor effect in combination with high dose paclitaxel in pancreatic carcinoma *in vivo*

Considering the high efficacy of the third-generation SB-Ts demonstrated *in vitro* and the previously reported systemic toxicity of second-generation SB-Ts *in vivo*,[16] we selected SB-T-121605 and 121606 for the analysis of antitumor effects and comparison to PTX *in vivo*. Cell-derived xenograft (CDX) Paca-44 mouse models were generated and treated with PTX alone or with combination regimens of PTX and SB-Ts. The following groups were used: 1) 4.5% DMSO in sterile water (control group), 2) 10 mg/kg PTX, 3) 9 mg/kg PTX and 1 mg/kg SB-T-121605, 4) 7 mg/kg PTX and 3 mg/kg SB-T-121605, 5) 9 mg/kg PTX and 1 mg/kg SB-T-121606, and 6) 7 mg/kg PTX and 3 mg/kg SB-T-121606. After two weeks of peritoneal applications of the above-specified regimens (two applications per week), a higher antitumor effect of combination regimens compared to PTX administered alone was found, although the trend was not statistically significant ($p = 0.058$). As expected, an uncontrolled and exponential growth of tumors in the control group and growth inhibition in the group with conventional PTX alone was observed (Figure 5A). Combination of PTX and SB-T-121606 had the fastest onset of a statistically significant effect for both tested concentrations already after the second application ($p = 0.022$) compared to the untreated control group. The most promising results were observed in combinations composed of PTX and 3 mg/kg SB-T-121605 ($p = 0.018$) or SB-T-121606 ($p = 0.032$). However, animals treated with combination regimens containing 1 and 3 mg/kg of SB-T-121605 or 3 mg/kg SB-T-121606 suffered with apparent weight loss, bowel obstruction, and overall physical wasting (Figure 5B). Due to a high standard deviation, the comparison of combination regimens and PTX alone was not statistically significant. Taking into account both the overall antitumor efficacy and adverse side effects, the most successful regimen seemed the combination of 1 mg/kg SB-T121606 with 9 mg/kg PTX.

Hematoxylin-eosin histopathology examination confirms effect of SB-Ts

Tumor tissue samples obtained from mice belonging to the treatment and control groups were fixed in RNAlater and stored at −70°C. They were histologically analyzed after further formalin fixation and paraffin embedding. Basic tissue morphology in hematoxylin-eosin stained slides was done, enabling clear differentiation between tumor and non-neoplastic tissue components. It should be noted that the chromatin of tumor cell nuclei was smudged, most likely due to RNAlater used as the original fixative. Tumor cells in all samples exhibited obvious nuclear enlargement. They formed thin anastomosing trabecules with interwoven desmoplastic stroma. Most tumors treated with taxanes exhibited partial regressive changes, consisting of geographic necrosis, adjacent fibrosis, and hemosiderin accumulation. The control sample also showed areas of necrosis, which on the other hand, may be due to rapid tumor growth. (Figure 6).

DISCUSSION

PDAC therapy remains problematic and frequently unsuccessful due to late diagnosis, chemoresistance, lack of targeted therapeutics, disease heterogeneity, and other reasons.[1,17] Limited drug penetration into the tumor due to dense stromal tissue is probably the main reason for chemoresistance.[18] mFOLFIRINOX is the therapeutic regimen of choice in patients with a high performance status but also causes more serious side effects than gemcitabine combined with taxanes or gemcitabine alone.[8] Therefore, it is imperative to search for the most effective drugs and modified therapeutic regimens with the best possible benefit-to-risk ratio. Here, we report the first findings of *in vitro* and *in vivo* efficacy testing of experimental SB-Ts in comparison to conventional PTX in PDAC models. The present study greatly expands our previous findings.[14]

Firstly, we confirmed that IC_{50} values for SB-Ts are lower than for PTX *in vitro* in PDAC cell lines with different *KRAS* mutation status. The data about second-generation SB-Ts cytotoxicity were published for the first time in the PTX-resistant ovarian carcinoma cell line NCI/ADR-RES and Adriamycin-sensitive breast carcinoma cell line MDA-MB-435.[19] The IC_{50} values for SB-Ts were comparable to docetaxel for MDA-MB-435 or lower than that of PTX for both used cell lines. PTX and docetaxel exhibited a significantly higher IC_{50} concentrations in NCI/ADR-RES cells compared to MDA–MB-435 [19]. In agreement with previous data on NCI/ADR-RES, the cytostatic effect of SB-T-121606 was high also in the Paca-44 cells (carrying *KRAS* G12V and *TP53* C176S mutations) and BxPC-3 cells (*KRAS* wild type) used in the present study

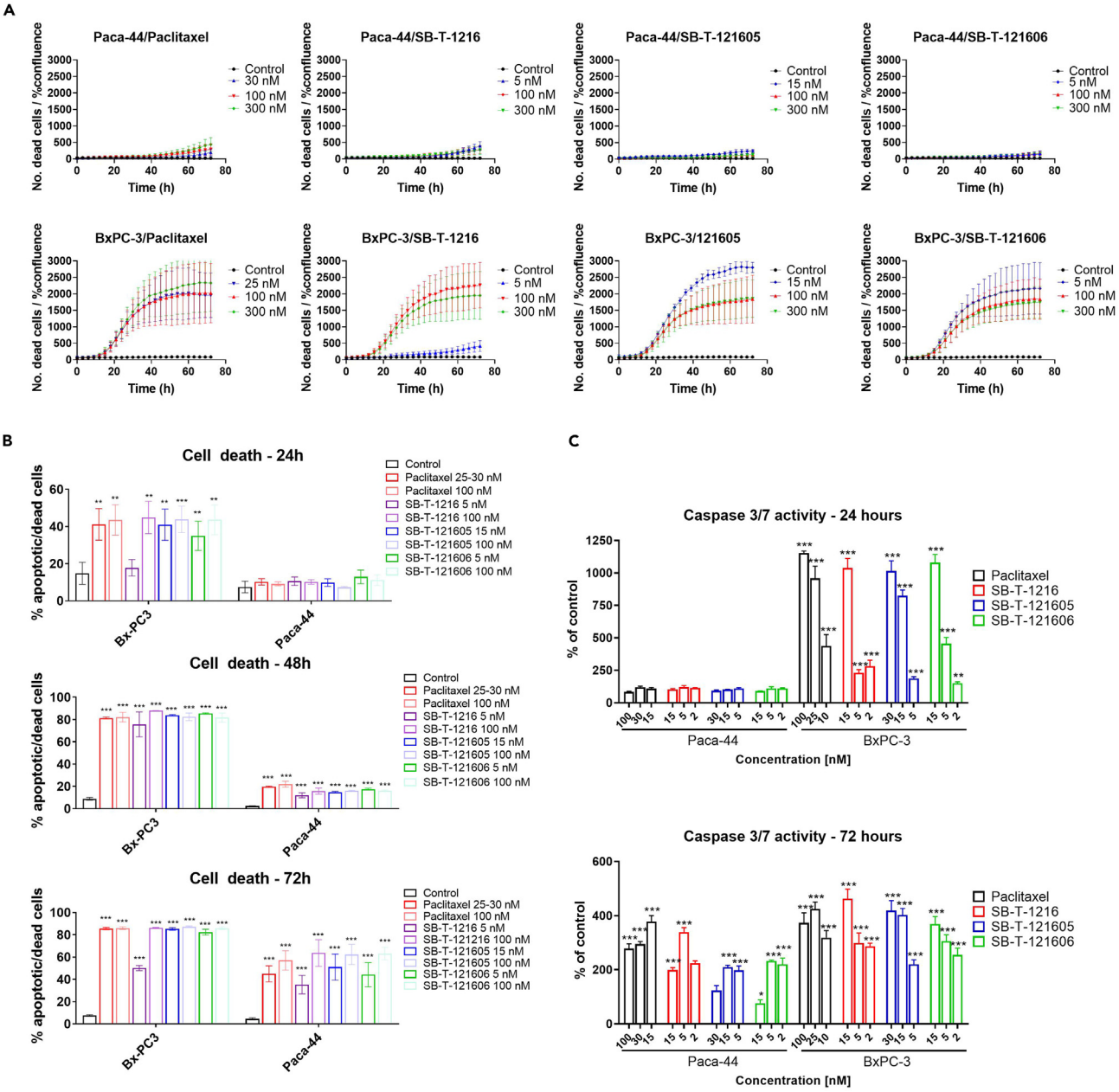

Figure 4. The analysis of cell death

(A) Real-time monitoring by SYTOX Green with concentrations corresponding to IC_{50} values (5–30 nM differing for each taxane-cell line combination), 100 and 300 nM PTX and SB-Ts. The data represent mean ± SD of three independent measurements.

(B) The analysis of cell death by Annexin V and propidium iodide after 24, 48, and 72 h of incubation of cells with IC_{50} and 100 nM concentrations of each taxane. All data presented as mean ± standard deviation. *p < 0.05, **p < 0.01, ***p < 0.001.

(C) Caspase 3 and 7 activity after 24 and 72 h of Paca-44 and BxPC-3 cells incubation with PXT and SB-Ts. Data are displayed as % of caspase activity in control cells incubated with cultivation medium only. All data presented as mean ± standard deviation. *p < 0.05, **p < 0.01, ***p < 0.001.

and approximately 8-times and 4-times higher than for PTX in Paca-44 and BxPC-3 cell line, respectively. Despite the third-generation SB-Ts having been synthesized with the goal of a higher efficacy compared to the second-generation, the SB-T-121605 is less effective than its predecessor SB-T-1216 in both cell lines evaluated in the *in vitro* part of this study. The observed results are thus different from our prior investigation on NCI/ADR-RES ovarian cancer cells where second-generation SB-Ts were less effective compared to their third-generation counterparts.[14] It should be the subject of follow-up studies to find out the reasons for this discrepancy and guide the next phase of drug development.

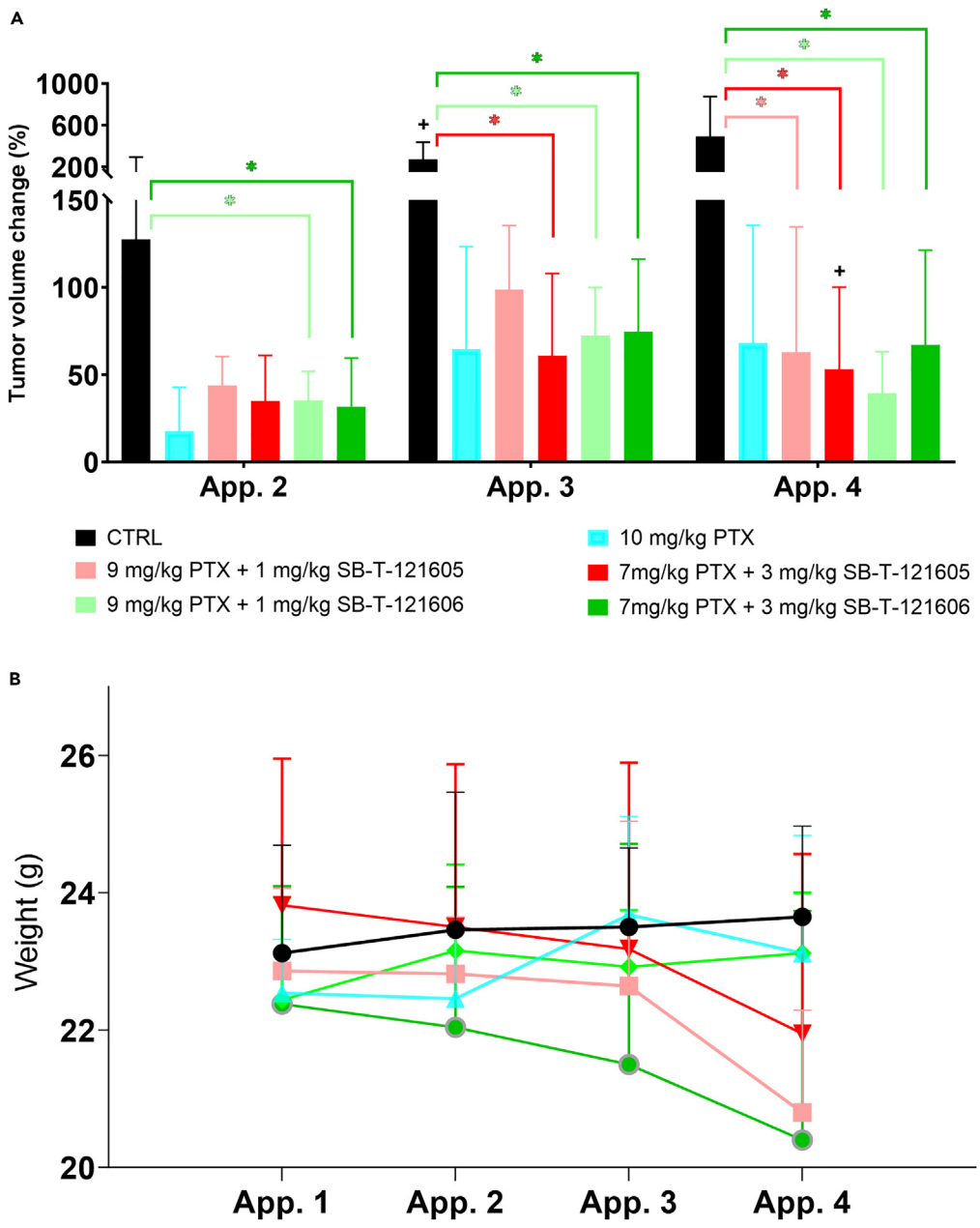

Figure 5. Comparison of tumor volume percentage change and body weight changes after administration of paclitaxel and SB-Ts *in vivo*

(A) Tumor volume change in percentage.

(B) Animal body weight in g measured after each application. Mean ± standard deviation presented for groups having five mice each at the beginning. *p-values by two-tailed Student's *t* test ($p \leq 0.05$). +Represents the death of animal in the group (one in the control group and one in 7 mg/kg PTX with 3 mg/kg SB-T-121605 group).

Subsequently, we analyzed changes in cell cycle, induction of cell death, PARP cleavage, and caspase 3/7 activation. Our investigations revealed that the decrease in viability of BxPC-3 and Paca-44 cell lines following taxane treatment is not directly linked to caspase-driven cell death. Interestingly, third generation SB-Ts exhibited induced cell death to the highest extent in the lowest concentration tested in the BxPC-3 cell line. Additionally, in the Paca-44 cell line, higher caspase activity was detected at low to intermediate compared to high concentrations tested, suggesting a differential sensitivity to the drug. This observation implies that lower concentrations of SB-Ts might be sufficient to induce significant therapeutic effects in certain tumor cells, potentially reducing the risk of side effects associated with higher doses. The data from the caspase 3/7 assay indicated no activation of caspase 3/7 in Paca-44 cell line after 24 h of incubation and this activation appeared after 72 h. This leads us to believe that the observed decline in viability could be attributed more likely to cytostatic rather than cytotoxic effects in

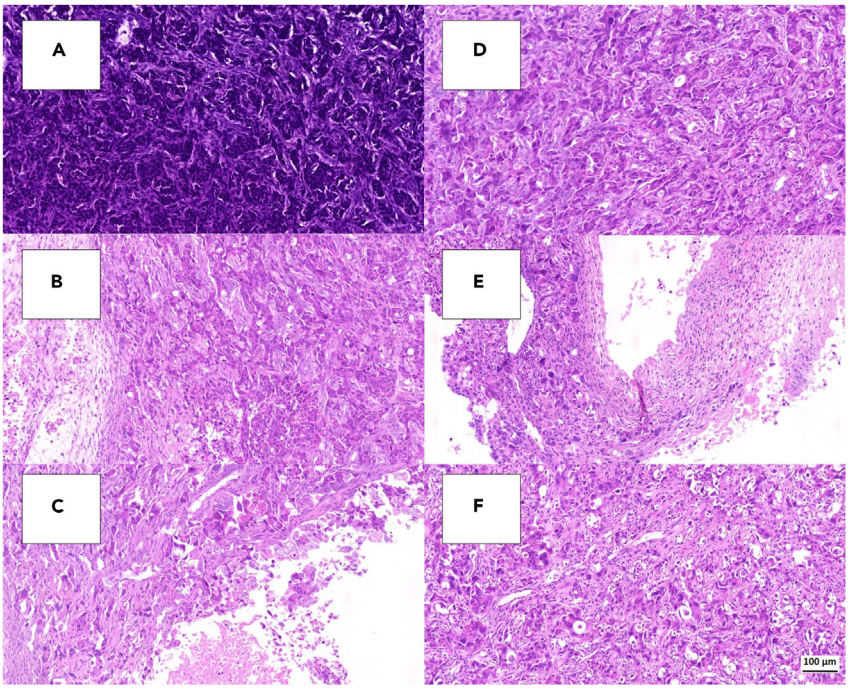

Figure 6. Hematoxylin-eosin histopathology examination of tumor tissues after administration of paclitaxel and SB-Ts *in vivo*

Tumor tissue samples were fixed in 4% neutral buffered formalin overnight and embedded in paraffin. Tissue blocks were sectioned in a microtome and stained with hematoxylin and eosin. Tumor morphology was assessed by a surgical pathologist.

(A) 4.5% DMSO in sterile water (control group).

(B) 10 mg/kg PTX.

(C) 9 mg/kg PTX and 1 mg/kg SB-T-121605.

(D) 7 mg/kg PTX and 3 mg/kg SB-T-121605.

(E) 9 mg/kg PTX and 1 mg/kg SB-T-121606.

(F) 7 mg/kg PTX and 3 mg/kg SB-T-121606. Magnification 200x, scale bar 100 µm is shown in the right bottom corner.

Paca-44 cells when compared to BxPC-3 cells. Additionally, the use of SYTOX Green for real-time cell death analysis corroborates our hypothesis. This analysis revealed that while the BxPC-3 cell line undergoes cell death within the first 24 h of exposure to the test compounds, the Paca-44 cell line shows similar effects only after roughly 72 h. Based on these findings, we propose that taxanes primarily exert a cytostatic effect on the Paca-44 cell line, inhibiting cell proliferation rather than triggering direct cell death, which makes Paca-44 less sensitive to taxane treatment when compared to BxPC-3 cells. This phenomenon may, at least in part, be related to the fact that the Paca-44 cell line carries a mutation in *KRAS*. These data fit with the results of a previous study where the BxPC-3 cell line manipulated to express the G12V mutant *KRAS* showed reduced levels of cell death in response to docetaxel and 5-fluorouracil compared to a *KRAS* wild-type parental subline.[15]

Finally, we explored the antitumor efficacy and systemic toxicity of third-generation SB-Ts combined with PTX in comparison with PTX alone in the mouse CDX Paca-44 model *in vivo*. In this pivotal experiment, we demonstrated that the combination of a high dose of conventional PTX with a low dose of the third-generation SB-T is very effective combination regimen. In line with our previous *in vitro* and *in vivo* observations of increased systemic toxicity of high doses of third-generation SB-Ts in monotherapy,[14] we used their low dose combination with a high-dose PTX, which is relatively safe. This adjustment allowed us to follow the "three R" principles in animal research, especially aimed at the reduction of the number of animals and refinement, because the high toxicity of monotherapy of SB-Ts could be avoided. The efficacy of second-generation SB-Ts *in vivo* in a spontaneous transplantable rat T cell lymphoma model was described earlier[16] and corroborated further in different models, including human PDAC CDX Paca-44 [12,13]. Thus, the present data further substantiate the efficacy of SB-Ts by demonstrating the well-tolerated activity of their third-generation in the Paca-44 pancreatic murine CDX model.

The Paca-44 cell line represents PDAC with the second most frequent *KRAS* G12V mutation seen in patient tumors and as such is suitable for research on targeted therapies.[20,21] It would be of great interest to combine SB-Ts with some of the compounds targeting *KRAS* mutations, especially the most frequently occurring ones.[22]

In general, SB-Ts are able to overcome the resistance to conventional taxanes such as PTX caused by, e.g., mutations in β-tubulin[23] or overexpression of P-glycoprotein (the case of NCI/ADR-RES cell line[24]) and can specifically target tumor-initiating or cancer stem cells.[25] Recently, the nanoemulsion formulation of second-generation SB-T conjugated to docosahexaenoic acid (NE-DHA-SBT-1214) showed great promise in preclinical studies of colorectal cancer and combination with PD-L1 antibodies also in pancreatic cancer.[26] Furthermore, we plan to compare efficacy of albumin-bound SB-Ts with nab-PTX used in PDAC patients with worse performance status.[8]

In conclusion, this study demonstrates the *in vitro* efficacy of conventional PTX and the newly synthesized second- (SB-T-1216) and third- (SB-T-121605 and SB-T-121606) generation taxanes in Paca-44 and BxPC-3 cell line models of human PDAC. Most importantly, the high antitumor effects of third-generation SB-Ts were confirmed *in vivo* by the Paca-44 CDX mouse model. Furthermore, the combination of high-dose PTX with low-dose third-generation SB-T-121606 had fast and long-lasting antitumor effects and tolerable systemic toxicity. Thus, third-generation SB-T-121605, and especially SB-T-121606 are promising candidates for the next phase of preclinical testing in combination with conventional chemotherapeutics in this highly aggressive and fatal malignancy.

Limitations of the study

Our study has certain limitations. We had to terminate the *in vivo* experiment after four cycles of administration of experimental compounds because of uncontrolled tumor growth in the nontherapeutic control group. This decision was done to maximally reduce the pain and distress of animals and because there were obvious positive effects in therapeutic groups. It is yet another proof of the aggressiveness, fast progression, and therefore suitability of this model for testing of experimental treatments. Another drawback of our approach is that PDAC is histologically and clinically highly different from ovarian or breast cancers, which we used as a pilot of this study design and thus these results, may not be fully comparable. Nevertheless, the side effects on the whole organism level remain the same, and the efficacy of treatment regimens containing SB-Ts encourages further preclinical research. We observed some statistically significant results, but statistical evaluation, in this case is challenging due to the work with animals and individually growing tumors being source of extreme variability. This high standard deviation is also the cause of statistically nonsignificant comparisons between PTX alone and combination regimens. Increasing the number of animals for purely statistical reasons would cause conflicts with the above mentioned 3R principle. On the other hand, despite the relatively large standard deviation of tumor size within each group, trends of tumor growth between groups are apparent and support the previous observations on a different model.[14] We realize that using subcutaneous CDX models with intraperitoneal therapeutics administration has its limitations also in the lack of clonal heterogeneity and limited interaction of tumor cells with the microenvironment. Therefore, we are currently testing the above substances and regimens in patient-derived xenografts (PDX) and we plan to extend the program by orthotopic models.

STAR★METHODS

Detailed methods are provided in the online version of this paper and include the following:

- KEY RESOURCES TABLE
- RESOURCE AVAILABILITY
  - Lead contact
  - Materials availability
  - Data and code availability
- EXPERIMENTAL MODEL AND STUDY PARTICIPANT DETAILS
  - Cell line and culture conditions
  - Cell line-derived xenograft *in vivo* model
- METHOD DETAILS
  - Materials
  - Cell growth and viability
  - Real-time monitoring of cell proliferation and death
  - Detection and quantification of cell death by Annexin V
  - Analysis of cell cycle
  - Caspase 3/7 activity analysis
  - Western blot analysis
  - Histopatology examination
- QUANTIFICATION AND STATISTICAL ANALYSIS

SUPPLEMENTAL INFORMATION

Supplemental information can be found online at https://doi.org/10.1016/j.isci.2024.109044.

ACKNOWLEDGMENTS

This work was supported by the Czech Medical Council project no. NV19-08-00113 (to P.S. and M.O.), the Czech Ministry of Education, Youth and Sports, INTER-ACTION project no. LUAUS23164 (to J.T. and V.N.), the National Institute for Cancer Research (NICR) project no. LX22NPO5102 financed by the European Union – Next Generation EU as part of the Czech Recovery Plan (to P.S.), the Grant Agency of the Czech Republic project no. 21-14082S (to R.V.), the Grant Agency of Charles University programs Cooperatio "Medical Diagnostics and Basic Medical Sciences" no. 207036 (to A.Sz.) and Donatio Facultatis Medicae Tertiae (to T.S.), and the National Institutes of Health (NIH), U.S.A. grant R01 CA103314 (to I.O.).

AUTHOR CONTRIBUTIONS

Conceptualization – R.V., L.C., I.O., M.O., and P.S.
Methodology – T.S., R.V., M.E., V.N., and J.T.
Validation – T.S., M.E., and C.S.A.
Formal Analysis – T.S., A.S., K.S., V.N., and J.T.
Investigation – T.S., S.B., A.S., K.S., M.E., K.K., C.S.A., and T.T.
Resources – R.V., J.T., L.C., I.O., and P.S.
Writing – Original Draft – T.S., R.V., and A.S.
Writing – Review and Editing – T.S., S.B., R.V., A.S., K.S., M.E., K.K., J.T., C.S.A., V.N., A.Sz., T.T., L.C., I.O., M.O., and P.S.
Visualization – T.S., A.S., M.E., A.Sz., and C.S.A.
Supervision –R.V., J.T., M.O., and P.S.
Project Administration – R.V. and P.S.
Funding Acquisition – T.S, R.V., L.C., I.O., M.O., and P.S.

DECLARATION OF INTERESTS

The authors declare no competing interests.

Received: July 13, 2023
Revised: December 4, 2023
Accepted: January 23, 2024
Published: January 26, 2024

REFERENCES

1. Rahib, L., Smith, B.D., Aizenberg, R., Rosenzweig, A.B., Fleshman, J.M., and Matrisian, L.M. (2014). Projecting cancer incidence and deaths to 2030: The unexpected burden of thyroid, liver, and pancreas cancers in the united states. Cancer Res. *74*, 2913–2921. https://doi.org/10.1158/0008-5472.CAN-14-0155.
2. Boursi, B., Finkelman, B., Giantonio, B.J., Haynes, K., Rustgi, A.K., Rhim, A.D., Mamtani, R., and Yang, Y.X. (2017). A Clinical Prediction Model to Assess Risk for Pancreatic Cancer Among Patients With New-Onset Diabetes. Gastroenterology *152*, 840–850.e3. https://doi.org/10.1053/j.gastro.2016.11.046.
3. Carr, R.M., and Fernandez-Zapico, M.E. (2016). Pancreatic cancer microenvironment, to target or not to target? EMBO Mol. Med. *8*, 80–82. https://doi.org/10.15252/emmm.201505948.
4. McGuigan, A., Kelly, P., Turkington, R.C., Jones, C., Coleman, H.G., and McCain, R.S. (2018). Pancreatic Cancer: A Review of Clinical Diagnosis, Epidemiology, Treatment and Outcomes. World J. Gastroenterol. *24*, 4846–4861. https://doi.org/10.3748/wjg.v24.i43.4846.
5. GBD 2017 Pancreatic Cancer Collaborators (2019). The global, regional, and national burden of pancreatic cancer and its attributable risk factors in 195 countries and territories, 1990–2017: a systematic analysis for the Global Burden of Disease Study 2017. Lancet. Gastroenterol. Hepatol. *4*, 934–947. https://doi.org/10.1016/S2468-1253(19)30347-4.
6. Waters, A.M., and Der, C.J. (2018). KRAS: The critical driver and therapeutic target for pancreatic cancer. Cold Spring Harb. Perspect. Med. *8*, a031435. https://doi.org/10.1101/cshperspect.a031435.
7. Mizrahi, J.D., Surana, R., Valle, J.W., and Shroff, R.T. (2020). Pancreatic cancer. Lancet *395*, 2008–2020. https://doi.org/10.1016/S0140-6736(20)30974-0.
8. Janssen, Q.P., Van Dam, J.L., Doppenberg, D., Prakash, L.R., Van Eijck, C.H.J., Jarnagin, W.R., O' Reilly, E.M., Paniccia, A., Besselink, M.G., Katz, M.H.G., et al. (2022). FOLFIRINOX as Initial Treatment for Localized Pancreatic Adenocarcinoma: A Retrospective Analysis by the Trans-Atlantic Pancreatic Surgery Consortium. J. Natl. Cancer Inst. *114*, 695–703. https://doi.org/10.1093/jnci/djac018.
9. Rogers, J.E., Mizrahi, J.D., Xiao, L., Mohindroo, C., Shroff, R.T., Wolff, R., Varadhachary, G.R., Javle, M.M., Overman, M., Fogelman, D.R., et al. (2020). Modified gemcitabine plus nab-paclitaxel regimen in advanced pancreatic ductal adenocarcinoma. Cancer Med. *9*, 5406–5415. https://doi.org/10.1002/cam4.3229.
10. Alqahtani, F.Y., Aleanizy, F.S., El Tahir, E., Alkahtani, H.M., and AlQuadeib, B.T. (2019). Paclitaxel. In Profiles of Drug Substances, Excipients and Related Methodology (Academic Press Inc), pp. 205–238. https://doi.org/10.1016/bs.podrm.2018.11.001.
11. Ojima, I., and Das, M. (2009). Recent advances in the chemistry and biology of new generation taxoids. J. Nat. Prod. *72*, 554–565. https://doi.org/10.1021/np8006556.
12. Mohelnikova-Duchonova, B., Kocik, M., Duchonova, B., Brynychova, V., Oliverius, M., Hlavsa, J., Honsova, E., Mazanec, J., Kala, Z., Ojima, I., et al. (2017). Hedgehog pathway overexpression in pancreatic cancer is abrogated by new-generation taxoid SB-T-1216. Pharmacogenomics J. *17*, 452–460. https://doi.org/10.1038/tpj.2016.55.
13. Oliverius, M., Flasarova, D., Mohelnikova-Duchonova, B., Ehrlichova, M., Hlavac, V., Kocik, M., Strouhal, O., Dvorak, P., Ojima, I., and Soucek, P. (2019). KRAS pathway expression changes in pancreatic cancer models by conventional and experimental taxanes. Mutagenesis *34*, 403–411. https://doi.org/10.1093/mutage/gez021.
14. Seborova, K., Koucka, K., Spalenkova, A., Holy, P., Ehrlichova, M., Sychra, T., Chen, L., Bendale, H., Ojima, I., Sandoval-Acuña, C., et al. (2022). Anticancer regimens containing third generation taxanes SB-T-121605 and SB-T-121606 are highly effective in resistant ovarian carcinoma model. Front. Pharmacol. *13*, 971905. https://doi.org/10.3389/fphar.2022.971905.
15. Geng, F., Tang, L., Li, Y., Yang, L., Choi, K.S., Kazim, A.L., and Zhang, Y. (2011). Allyl isothiocyanate arrests cancer cells in mitosis, and mitotic arrest in turn leads to apoptosis via Bcl-2 protein phosphorylation. J. Biol. Chem. *286*, 32259–32267. https://doi.org/10.1074/jbc.M111.278127.
16. Otová, B., Ojima, I., Václavíková, R., Hrdý, J., Ehrlichová, M., Souček, P., Vobořilová, J., Němcová, V., Zanardi, I., Horský, S., et al. (2012). Second-generation taxanes effectively suppress subcutaneous rat lymphoma: Role of disposition, transport, metabolism, in vitro potency and expression of angiogenesis genes. Invest. New Drugs *30*, 991–1002. https://doi.org/10.1007/s10637-011-9654-0.
17. Park, W., Chawla, A., and O'Reilly, E.M. (2021). Pancreatic Cancer: A Review. JAMA *326*, 851–862. https://doi.org/10.1001/jama.2021.13027.
18. Pandey, V., and Storz, P. (2019). Targeting the tumor microenvironment in pancreatic ductal adenocarcinoma. Expert Rev. Anticancer Ther. *19*, 473–482. https://doi.org/10.1080/14737140.2019.1622417.
19. Ehrlichova, M., Vaclavikova, R., Ojima, I., Pepe, A., Kuznetsova, L.V., Chen, J., Truksa, J., Kovar, J., and Gut, I. (2005). Transport and cytotoxicity of paclitaxel, docetaxel, and novel taxanes in human breast cancer cells. Naunyn-Schmiedeberg's Arch. Pharmacol. *372*, 95–105. https://doi.org/10.1007/s00210-005-1080-4.
20. Buscail, L., Bournet, B., and Cordelier, P. (2020). Role of oncogenic KRAS in the diagnosis, prognosis and treatment of

pancreatic cancer. Nature Res. *17*, 153–168. https://doi.org/10.1038/s41575-019-0245-4.

21. Hayashi, A., Hong, J., and Iacobuzio-Donahue, C.A. (2021). The pancreatic cancer genome revisited. Nature Res. *18*, 469–481. https://doi.org/10.1038/s41575-021-00463-z.
22. Kemp, S.B., Cheng, N., Markosyan, N., Sor, R., Kim, I.-K., Hallin, J., Shoush, J., Quinones, L., Brown, N.V., Bassett, J.B., et al. (2023). Efficacy of a Small-Molecule Inhibitor of KrasG12D in Immunocompetent Models of Pancreatic Cancer. Cancer Discov. *13*, 298–311. https://doi.org/10.1158/2159-8290.CD-22-1066.
23. Matesanz, R., Trigili, C., Rodríguez-Salarichs, J., Zanardi, I., Pera, B., Nogales, A., Fang, W.-S., Jímenez-Barbero, J., Canales, Á., Barasoain, I., et al. (2014). Taxanes with high potency inducing tubulin assembly overcome tumoural cell resistances. Bioorg. Med. Chem. *22*, 5078–5090. https://doi.org/10.1016/j.bmc.2014.05.048.
24. Ehrlichová, M., Ojima, I., Chen, J., Václavíková, R., Němcová-Fürstová, V., Vobořilová, J., Šimek, P., Horský, S., Souček, P., Kovář, J., et al. (2012). Transport, metabolism, cytotoxicity and effects of novel taxanes on the cell cycle in MDA-MB-435 and NCI/ADR-RES cells. Naunyn-Schmiedeberg's Arch. Pharmacol. *385*, 1035–1048. https://doi.org/10.1007/s00210-012-0785-4.
25. Botchkina, G.I., Zuniga, E.S., Das, M., Wang, Y., Wang, H., Zhu, S., Savitt, A.G., Rowehl, R.A., Leyfman, Y., Ju, J., et al. (2010). New-generation taxoid SB-T-1214 inhibits stem cell-related gene expression in 3D cancer spheroids induced by purified colon tumor-initiating cells. Mol. Cancer *9*, 192. https://doi.org/10.1186/1476-4598-9-192.
26. Ahmad, G., Mackenzie, G.G., Egan, J., and Amiji, M.M. (2019). DHA-SBT-1214 Taxoid Nanoemulsion and Anti–PD-L1 Antibody Combination Therapy Enhances Antitumor Efficacy in a Syngeneic Pancreatic Adenocarcinoma Model. Mol. Cancer Ther. *18*, 1961–1972. https://doi.org/10.1158/1535-7163.MCT-18-1046.
27. Ojima, I., Chen, J., Sun, L., Borella, C.P., Wang, T., Miller, M.L., Lin, S., Geng, X., Kuznetsova, L., Qu, C., et al. (2008). Design, synthesis, and biological evaluation of new-generation taxoids. J. Med. Chem. *51*, 3203–3221. https://doi.org/10.1021/jm800086e.
28. Seitz, J.D., Wang, T., Vineberg, J.G., Honda, T., and Ojima, I. (2018). Synthesis of a Next-Generation Taxoid by Rapid Methylation Amenable for 11C-Labeling. J. Org. Chem. *83*, 2847–2857. https://doi.org/10.1021/acs.joc.7b03284.
29. Seitz, J.D., Vineberg, J.G., Herlihy, E., Park, B., Melief, E., and Ojima, I. (2015). Design, synthesis and biological evaluation of a highly-potent and cancer cell selective folate-taxoid conjugate. Bioorg. Med. Chem. *23*, 2187–2194. https://doi.org/10.1016/j.bmc.2015.02.057.
30. Sychra, T., Václavíková, R., Szabó, A., Spálenková, A., Šeborová, K., Balatka, Š., Tesařová, T., Kočí, K., Gürlich, R., Souček, P., and Oliverius, M. (2022). Introducing in vivo pancreatic cancer models for the study of new therapeutic regimens. Rozhl. Chir. *101*, 584–592. https://doi.org/10.33699/PIS.2022.101.12.584-592.

STAR★METHODS

KEY RESOURCES TABLE

REAGENT or RESOURCE	SOURCE	IDENTIFIER
Chemicals, peptides, and recombinant proteins		
SB-T-1216	Stony Brook University, 100 Nicolls Rd, Stony Brook, NY 11794, NY, USA	https://doi.org/10.1002/(SICI)1520-636X(2000)12:5/6<431::AID-CHIR24>3.0.CO;2-M
SB-T-121605	Stony Brook University, 100 Nicolls Rd, Stony Brook, NY 11794, NY, USA	https://doi.org/10.1021/jm800086e
SB-T-121606	Stony Brook University, 100 Nicolls Rd, Stony Brook, NY 11794, NY, USA	https://doi.org/10.1021/jm800086e
Experimental models: Cell lines		
BxPC3	Cell Lines Service GmbH Company, Eppelheim, Baden- Dr.-Eckener-Str. 8, Eppelheim, Baden-Württemberg, 69214, Germany	Product number: 305031
Paca-44	Leibniz Institute; DSMZ-German Collection of Microorganisms and Cell Cultures GmbH, Inhoffenstraβe 7B, Braunschweig; Science Campus Braunschweig-Süd, 38124, Germany	PA-TU-8902, cat. no. ACC 179
Experimental models: Organisms/strains		
Athymic Nude mice, Crl:NU(NCr)-Foxn1nu	Charles River Laboratories Germany GmbH, Am Flughafen 12, Freiburg im Breisgau, 79108, Germany	https://www.criver.com/products-services/find-model/athymic-nude-mouse?region=3616

RESOURCE AVAILABILITY

Lead contact

Further information and requests for resources and reagents should be directed to and will be fulfilled by the lead contact, Pavel Soucek (pavel.soucek@szu.cz).

Materials availability

This study did not generate new unique reagents.[11,27–29]

Data and code availability

- All data reported in this paper will be shared by the lead contact upon reasonable request.
- This paper does not report original code.

EXPERIMENTAL MODEL AND STUDY PARTICIPANT DETAILS

Cell line and culture conditions

Two human PDAC cell line models were included in this study - Paca-44 and BxPC-3. Paca-44 (carrying *KRAS* G12V and *TP53* C176S mutations) was obtained from Leibniz Institute DSMZ-German Collection of Microorganisms and Cell Cultures, Braunschweig, Germany (product. no. ACC 179) and the BxPC-3 cell line (*KRAS* wild type) was obtained from CLS (Eppelheim, Germany, product no. 305031). Cells were cultured in RPMI 1640 medium with L-Glutamine (300 mg/L), $NaHCO_3$ (2 g/L), penicillin-streptomycin (penicillin 100 U/mL, streptomycin 100 µg/mL), sodium pyruvate (1 mM), HEPES (15 mM) and fetal bovine serum or heat-inactivated fetal bovine serum (PAN-Biotech, Aidenbach, Germany) at final concentration 10% for Paca-44 or BxPC-3 cells, respectively. The cell lines were cultured at 37°C in an incubator with a 5% CO_2 atmosphere. MycoAlert mycoplasma detection kit (Lonza, Basel, Switzerland) was used for regular mycoplasma contamination tests. The authenticity of the cells was checked by short tandem repeats (STR) DNA profiling analysis. For amplification of STR loci, a PowerPlex 16 System (Promega, Madison, WI, USA) was used according to the technical manual.

Cell line-derived xenograft *in vivo* model

All experiments with animals were performed by investigators possessing the authorization to work with experimental animals and carried out, implemented in compliance with, and governed by the existing regulations and guidelines for the breeding and experimental use of animals following Czech jurisdiction, Act No. 246/1992 Coll. on the protection of animals against cruelty, as amended. The study was approved by the Ministry of Health of the Czech Republic (approval no. 31/2018 of 15th May 2018).

Female immunodeficient strains of NU/NU mice (Athymic Nude mice, Crl:NU(NCr)-Foxn1nu) at 4–6 weeks of age, obtained in Charles River Laboratories (Freiburg, Germany), were used for the experiments at the Experimental Animal Welfare Department of the National Institute of Public Health in a specific pathogen-free environment. Animals were provided with feeding and water *ad libitum*. All interventions and measurements were done under general inhalation anesthesia of isoflurane (ISOFLURIN 1000 mg/g; Vetpharma Animal Health, S.L., Barcelona, Spain). Firstly, 3 × 10^6 Paca-44 cells in 100 μL of PBS were injected subcutaneously into the right dorsal quadrant of each animal's back. After the successful growth of tumors to at least 100 mm^3 (Figure S6), 30 CDX mice were divided into six groups consisting of five mice: 1) control group administered with only vehicle (4.5% DMSO in sterile water for cell culture, PAN-Biotech), 2) group treated with 10 mg/kg PTX, 3) group treated with a combination of 9 mg/kg PTX and 1 mg/kg SB-T-121605, 4) group treated with a combination of 7 mg/kg PTX and 3 mg/kg SB-T-121605, 5) group treated with a combination of 9 mg/kg PTX and 1 mg/kg SB-T-121606, and 6) group treated with a combination of 7 mg/kg PTX and 3 mg/kg SB-T-121606. Therapeutics were applied intraperitoneally in a total volume of 200 μL, twice a week, for two weeks. Based on our previous experiments, combinations of SB-Ts with conventional taxane were selected due to the higher toxicity of high-dose (>3 mg/kg) SB-Ts monotherapy.[14]

The change in animal body weight and tumor volume was monitored before each application. For the calculation of tumor volume, standard formula (width^2 x length)/2 was used. After four cycles of treatment, animals were sacrificed. The detailed methodology of handling experimental animals in our welfare animal lab, including photo documentation, can be found in publications.[13,14,30]

METHOD DETAILS

Materials

PTX used for *in vitro* experiments was obtained from Sigma Aldrich (St. Louis, MO, USA). An infusion solution of PTX (Paclitaxel EBEWE, 6 mg/mL, Ebewe Pharma, Unterach am Attersee, Austria) was used for the *in vivo* study. SB-Ts of the second (SB-T-1216) and third (SB-T-121605 and SB-T-121606) generation were synthesized at the Institute of Chemical Biology & Drug Discovery (Stony Brook University, Stony Brook, NY, USA) (Figure S1).[27] The design and synthesis were in detail described in studies previously published by Ojima and Seitz.[11,28,29] PTX and all SB-Ts stock solutions were dissolved in DMSO and their concentration was 10 mM. Working solutions were prepared just before use. The concentration of DMSO incubated with cells did not exceed 0.3%.

Cell growth and viability

Cells were seeded in a complete growth medium into a black 96-well plate at a concentration of 5 × 10^3 cells/well. After 18 h, the medium was replaced with a fresh growth medium with added PTX, SB-Ts, or pure medium as a control. The range of concentrations was 0.003–30 000 nM for PTX and all SB-Ts. The maximum concentration of DMSO was 0.3%. After 72 h of incubation, cell viability was evaluated by measuring fluorescence using the Infinite M200 (Tecan, Männedorf, Switzerland) along with a CellTiter-Blue viability assay (Promega) according to the manufacturer's instructions. All experiments were repeated three times.

Real-time monitoring of cell proliferation and death

An alternative approach to measure cell proliferation was performed by real-time monitoring of cells by the Incucyte SX3 microscope (Sartorius, Göttingen, Germany). Cells were seeded at 3 × 10^3 per well in a 96-well plate, left undisturbed overnight to attach to the surface, and the tested compounds were added the next day, together with SYTOX green dye (150 nM: Thermo Fisher Scientific) to stain dead cells. A picture of each well was taken every 3 h over a period of 72 h. Brightfield and green channel pictures were analyzed by the Incucyte software and the results expressed as percentage of confluence relative to time 0 for proliferation and number of dead cells over confluence for dead cells.

Detection and quantification of cell death by Annexin V

Cells were seeded in 12-well plates at a concentration of 1 × 10^5 cells/well and allowed to attach overnight. The next day, PTX (25 or 30 and 100 nM). SB-T-1216 (5 and 100 nM), SB-T-121605 (15 and 100 nM), or SB-T-121606 (5 and 100 nM) were added and the cells were incubated for 24, 48, or 72 h. After the treatment, cells were collected by trypsinization and stained with Annexin V (BioLegend, San Diego, CA, USA) for 30 min at 4°C. Finally, cells were stained with propidium iodide (0.5 μg/mL) and analyzed using a flow cytometer LSRFortessa (Becton Dickinson, Franklin Lakes, NJ, USA). A total of 10 000 cells/events were measured in each run. The raw data were analyzed using the FlowJo software (Becton Dickinson). All experiments were performed in three independent measurements.

Analysis of cell cycle

Cells were seeded in 6-well plates at a concentration of 1 × 10^5 cells or 2 × 10^5 cells/well for Paca-44 and BxPC-3, respectively, and allowed to attach overnight. The next day, PTX (25 or 30 and 100 nM), SB-T-1216 (5 and 100 nM), SB-T-121605 (15 and 100 nM), or SB-T-121606 (5 and 100 nM) were added and the cells were incubated for an additional 24 h. Finally, cells were harvested by trypsinization, fixed and

permeabilized with the Click-iT EdU kit (Thermo Fisher Scientific) and stained with Vybrant DyeCycle Violet Stain (Thermo Fisher Scientific) for 30 min at 37°C. The stained cells were analyzed using a flow cytometer LSRFortessa (Becton Dickinson). A total of 50 000 cells/events were measured in each run. The raw data were analyzed using the FlowJo software (Becton Dickinson). All experiments were performed in three independent measurements.

Caspase 3/7 activity analysis

5×10^3 cells/well were seeded onto a 96-well plate and allowed to adhere overnight. Subsequently, fresh medium (control), or medium with different concentrations of PTX, SB-T-1216, SB-T-121605, or SB-T-121606 was added. After 24 and 72 h of incubation, the activity of caspases 3/7 was evaluated by the Caspase-Glo 3/7 Assay System (Promega). The luminescence intensity was measured using the Infinite M200 instrument (Tecan). The activity was analyzed in triplicates.

Western blot analysis

Both cell lines were seeded at a density of 5×10^5 cells into 60 mm Petri dishes, followed by an overnight incubation. Next day, fresh medium (control) or medium containing PTX, SB-T-1216, SB-T-121605 or SB-T-121606 was added. Cells were harvested after 24 and 72 h of incubation by trypsinization, washed by PBS, centrifuged and resuspended in RIPA buffer (3% Triton X-, 10 mM HEPES, pH 7.4, 0.15 M NaCl, 5 mM EDTA) with cOmplete ULTRA Tablets and PhosSTOP Tablets (Roche, Basel, Switzerland). Protein lysates (15 μg of total proteins per sample) were mixed with sample buffer and denatured at 95°C for 8 min. Subsequently, proteins were separated on 12% polyacrylamide gels at 160 V and blotted onto 0.2 μm nitrocellulose membrane (Protran BA83, Schleicher-Schuell, Dassel, Germany) for 3 h at 0.25 A. The membranes were blocked in 5% weight/volume bovine serum albumin in Tris-buffered saline for 30 min at room temperature. The washed membranes were probed overnight at 4°C with following primary antibodies against cleaved caspase-3 (dilution 1:500, #9664, Cell Signaling), PARP (dilution 1:750, #9542, Cell Signaling), phospho-Bcl-2 (Ser70) (dilution 1:400, #2827, Cell Signaling) and actin (dilution 1:1500, clone AC-40, A4700, Sigma-Aldrich). After washing, the membranes were incubated for 2 h at room temperature with corresponding horseradish peroxidase-conjugated secondary antibodies (dilution 1:10 000; Proteintech). Protein bands were visualized with an enhanced chemiluminescence detection system (Thermo Fisher Scientific) using Alliance Q9 Chemiluminescence Imager (Uvitec). Densitometry was performed using the Image Lab 6.1 software (Biorad).

Histopatology examination

Tumor tissue samples procured after autopsy were stored at −70°C in RNAlater solution. After thawing, the samples were fixed in 4% neutral buffered formalin overnight and embedded in paraffin. Tissue blocks were sectioned in a microtome and stained with hematoxylin and eosin. Tumor morphology was assessed by experienced surgical pathologist.

QUANTIFICATION AND STATISTICAL ANALYSIS

IC_{50} values were evaluated by GraphPad Prism 9.5 (GraphPad Software, Boston, MA, USA) and are displayed as mean ± S.D. of three independent experiments. Caspase activity, protein expression, tumor volume, and weight of mice were analyzed by two-tailed Student's T-test in MS Excel and displayed by GraphPad Prism 9.5. P-values <0.05 were considered statistically significant.